

Frustration in  $R_2PdSi_3$  ( $R = Tb, Er$ ) compounds: spin-glass or magnetic short range order?  
Neutron diffraction studies

This article has been downloaded from IOPscience. Please scroll down to see the full text article.

2007 J. Phys.: Condens. Matter 19 145276

(<http://iopscience.iop.org/0953-8984/19/14/145276>)

View [the table of contents for this issue](#), or go to the [journal homepage](#) for more

Download details:

IP Address: 129.252.86.83

The article was downloaded on 28/05/2010 at 17:37

Please note that [terms and conditions apply](#).

# Frustration in $R_2PdSi_3$ ( $R = Tb, Er$ ) compounds: spin-glass or magnetic short range order? Neutron diffraction studies

M Frontzek<sup>1</sup>, A Kreyssig<sup>1</sup>, M Doerr<sup>1</sup>, A Schneidewind<sup>1,2</sup>, J-U Hoffmann<sup>3</sup>  
and M Loewenhaupt<sup>1</sup>

<sup>1</sup> Institut für Festkörperphysik, Technische Universität Dresden, D-01062 Dresden, Germany

<sup>2</sup> Forschungsneutronequelle Heinz Maier-Leibnitz, D-85747 Garching, Germany

<sup>3</sup> Hahn-Meitner Institut Berlin, D-01409 Berlin, Germany

Received 16 October 2006

Published 23 March 2007

Online at [stacks.iop.org/JPhysCM/19/145276](http://stacks.iop.org/JPhysCM/19/145276)

## Abstract

Measurements of macroscopic magnetic properties of the isostructural compounds  $Tb_2PdSi_3$  and  $Er_2PdSi_3$  show an additional phase transition below the ordering temperature. The behaviours of the two compounds are similar and are interpreted as spin-glass-like phase transitions in the literature.

In this contribution, we present detailed neutron diffraction studies of the mechanism of the spin-glass-like phase transition on a microscopic scale. We find a fundamental difference between the two compounds in their magnetic structures and, therefore, the spin-glass-like phase transitions. In the  $Tb_2PdSi_3$  compound an additional antiferromagnetic short range ordered phase is found within the long range ordered phase. The appearance of the short range order is linked to the spin-glass-like transition. In contrast, the  $Er_2PdSi_3$  compound shows only long range order. However, the antiferromagnetic order undergoes a modification within the ordered state. The temperature of the transition matches the spin-glass-like transition.

(Some figures in this article are in colour only in the electronic version)

## 1. Introduction

The series of  $R_2PdSi_3$  ( $R =$  rare earth) compounds has been a focus of interest for over 15 years [1]. The compounds crystallize in an  $A1B_2$ -derived hexagonal structure ( $P6/mmm$ ) with a latent geometric frustration. The magnetic rare-earth ions occupy the A1 positions of the  $A1B_2$  structure while the non-magnetic Pd and Si atoms are assumed to be statistically distributed on the B positions [2]. Most of the  $R_2PdSi_3$  ( $R = Ce, Gd, Tb, Dy, Ho, Er, Tm$ ) compounds order antiferromagnetically below Néel temperatures between 1.8 K (Tm) and 23.6 K (Tb) [1–3]. The  $Nd_2PdSi_3$  compound orders ferromagnetically below  $T_C = 17$  K [2].  $Tb_2PdSi_3$  ( $T_N = 23.6$  K)

and  $\text{Er}_2\text{PdSi}_3$  ( $T_N = 7.0$  K) are of special interest because they exhibit in addition a spin-glass-like (SGL) phase transition around  $T_2 \approx 8$  and 2 K, respectively [4, 5]. These SGL transitions were characterized predominantly with ac and dc susceptibility measurements. The ac susceptibilities of both compounds show a strong dependence of the transition temperature on the ac frequency. However, only for the  $\text{Tb}_2\text{PdSi}_3$  compound was a large difference between field cooling (FC) and zero-field cooling (ZFC) found in the dc susceptibility. This behaviour was attributed to a non-vanishing magnetization relaxing with a time dependence, that was interpreted as spin-glass behaviour [6]. The SGL transitions for both compounds were also attributed to geometrical frustration. The similarities in the ac susceptibilities lead to the assumption of identical mechanisms driving the spin-glass-like transition.

Previously, the magnetic structures were investigated using neutron diffraction on powder samples [2]. However, our data obtained from single-crystal neutron diffraction are in contradiction to the published magnetic structures. The magnetic structures determined from the single-crystal neutron diffraction data will be presented in a forthcoming publication and only those results that are necessary for the understanding of the SGL transition will be shown here. For the  $\text{Tb}_2\text{PdSi}_3$  compound it should be remarked that Szytula *et al* identified a spin-glass component from broad magnetic reflections near the Néel temperature [2]. With the knowledge of the positions of the magnetic reflections from single-crystal data [7] these broad peaks can also be interpreted as several distinct magnetic reflections smeared out by the limited instrumental resolution and powder averaging.

## 2. Experimental details

The single crystals were grown by floating zone melting with optical heating at temperatures  $> 1500^\circ\text{C}$  from polycrystalline rods of 6 mm diameter and 55 mm length [8, 9]. The resulting crystals were characterized by scanning electron microscopy and oriented using the x-ray Laue method. Cuboid shaped single crystals with a mass around 40 mg were primed for ac susceptibility measurements.

The ac susceptibility measurements were performed in an Oxford Instruments  $^4\text{He}$  discharge flow-through cryostat. The experimental parameters for the ac susceptibility measurements comprise an excitation field of 0.5 mT with a frequency range of 1 Hz–10 kHz.

The neutron scattering experiments were performed at Hahn-Meitner Institute (HMI) in Berlin and the FRM-II in Garching. The  $\text{Tb}_2\text{PdSi}_3$  ( $m = 463$  mg) and  $\text{Er}_2\text{PdSi}_3$  ( $m \approx 1300$  mg) single crystals used for the neutron diffraction studies were of high quality over the whole sample volume. Mapping of full reciprocal planes was done at the flat-cone E2 diffractometer at HMI with an incident wavelength of  $\lambda = 2.39$  Å. The detailed temperature dependence of the magnetic phase in  $\text{Tb}_2\text{PdSi}_3$  was studied at the cold three-axis PANDA spectrometer at the FRM-II with an incident wavelength of  $\lambda = 4.19$  Å.

## 3. Results

### 3.1. Frequency dependent ac susceptibility

The SGL transition for both compounds is characterized by a pronounced ac frequency dependence of the transition temperatures. Figure 1 shows the measurements with the ac field along the respective magnetic easy directions for each compound. The SGL transition can also be observed with an ac field along the magnetic hard direction but the susceptibility signal is small. The SGL transition at the respective temperature  $T_2$  features an intense and broad contribution in the imaginary part of the ac susceptibility for both compounds. The real

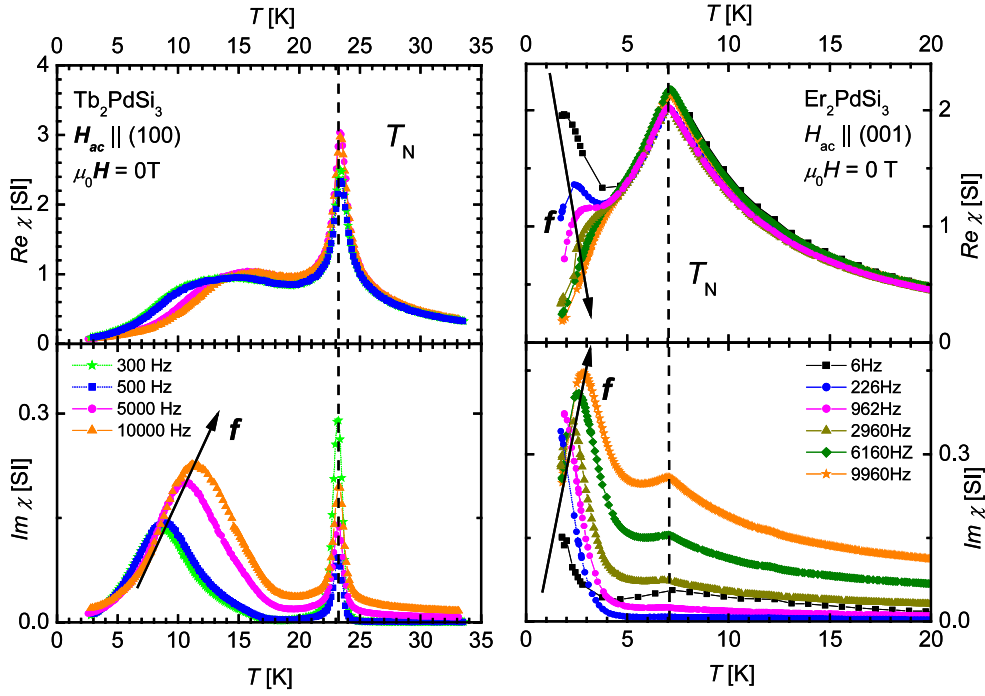


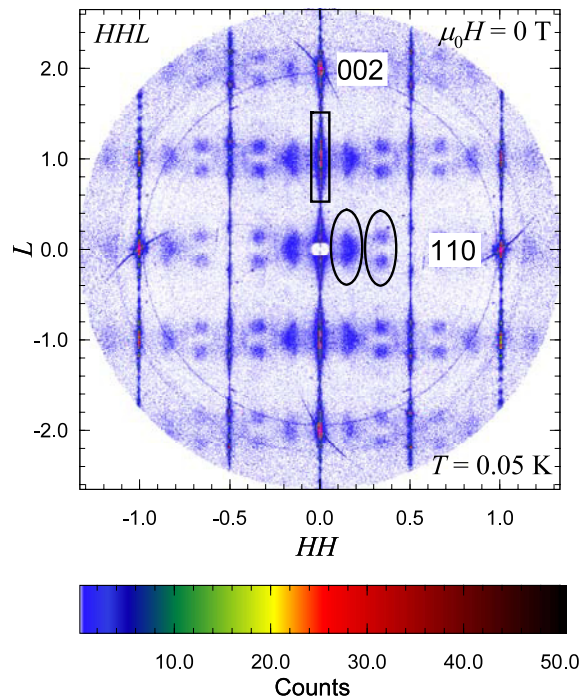
**Figure 1.** Real and imaginary parts of the ac susceptibility of  $\text{Tb}_2\text{PdSi}_3$  (left-hand side) and  $\text{Er}_2\text{PdSi}_3$  (right-hand side) measured at different ac frequencies (increasing in the direction of the arrow) with  $H_{ac}$  parallel to the respective easy axis of the compound.

part shows a negligible and a strong damping of the signal with increasing frequency for both  $\text{Tb}_2\text{PdSi}_3$  and  $\text{Er}_2\text{PdSi}_3$ .

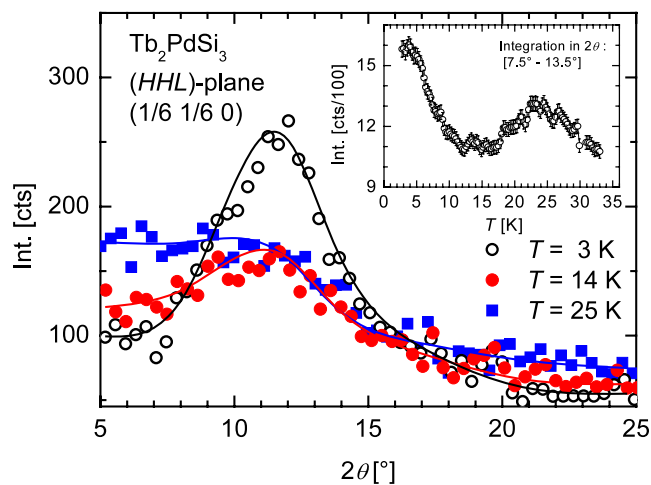
### 3.2. $\text{Tb}_2\text{PdSi}_3$ : neutron diffraction

Figure 2 shows a map of the reciprocal ( $HHL$ ) plane at  $T = 50$  mK. This reciprocal plane contains 10 nuclear reflections (001), (002), (110), and (111). Two rings originate from scattering on polycrystalline aluminium (sample holder, cryostat). The remaining intensity fades into the background above the Néel temperature and is, therefore, of magnetic origin.

The circles mark magnetic intensity due to short range antiferromagnetic order (SRO). The position of the SRO is  $1/6$  and  $2/6$  along the ( $HH0$ ) direction, while it is  $1/16$  and  $2/16$  along ( $00L$ ) assuming four magnetic reflections in the two marked circles. Figure 3 shows the magnetic intensity due to SRO measured at three different temperatures. At the lowest temperature ( $T = 3$  K) a broad peak is observed centred at approximately  $12^\circ$  in  $2\Theta$ . This value equals the position  $(1/6 \ 1/6 \ 0)$  in reciprocal space. The intensity on this position decreases with increasing temperature. However, magnetic intensity due to a fluctuating ferromagnetic moment component is measured near the position of the SRO. The ferromagnetic intensity is observed mainly around the origin and the (001) reflections. It is distinguishable from the background from around 14 K and has its maximum intensity around  $T_N$ . The integrated intensity (from  $7.5^\circ$  to  $13.5^\circ$  in  $2\Theta$ ) for the temperature range from 2 to 33 K is shown in the inset. The temperature dependence of the antiferromagnetic SRO (position  $(1/6 \ 1/6 \ 0)$ ) results in a characteristic temperature of  $T_2 \approx 8$  K. This correlates well with the temperature dependence of the SGL contribution in the imaginary ac susceptibility signal (see figure 1).



**Figure 2.** Map of the reciprocal  $HHL$  plane of  $Tb_2PdSi_3$  at  $T = 50$  mK. (002) and (110) nuclear reflections are marked. The magnetic intensity discussed in the article is pointed out by a box (LRO) and circles (SRO) respectively.



**Figure 3.** Magnetic intensity due to SRO at three different temperatures. The lines are guides to the eyes. The integrated raw data are shown in the inset.

Magnetic intensity due to a long range ordered antiferromagnetic (LRO) phase is found at positions  $(m/2 m/2 n/16)$  with  $m = 0, 1, 2, \dots$ , and  $n$  being an odd integer. In figure 2 the box selects a part of the LRO intensity which is shown in figure 4 as a section from  $(0 0 0.5)$  to  $(0 0 1.5)$ . This section shows the antiferromagnetic satellites originating from the nuclear (001)

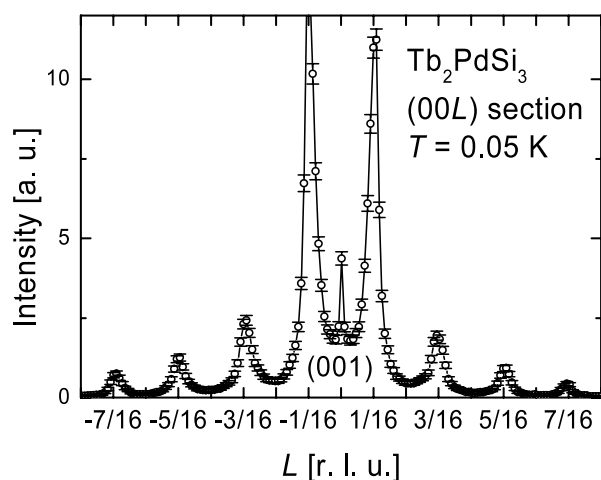


**Figure 4.** Section of the long range ordered magnetic structure extracted from the box marked area in figure 2.

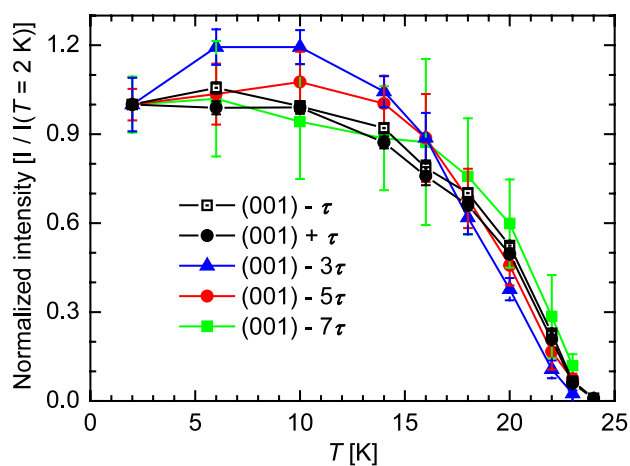


**Figure 5.** Normalized intensity for the different harmonics of the propagation vector of the magnetic LRO in  $\text{Tb}_2\text{PdSi}_3$ .

reflection. The positions of the reflections are  $(001 \pm n/16)$ . The intensity relation between the different harmonics corresponds to a squared-up modulation of the magnetic moments along the  $c$  axis. The magnetic structure doubles the chemical unit cell in the basal plane. The magnetic propagation vector is  $\tau = (001/16)$ . In agreement with the magnetization measurements, the intensity distribution indicates an alignment of the magnetic moments within the basal plane. A long range ordered ferromagnetic component is not observed.

The temperature dependence of the normalized magnetic intensity due to the LRO is drawn in figure 5. In contrast to the SRO case, the characteristic temperature of the LRO is  $T_N = 23$  K for all harmonics of the propagation vector. Furthermore, the normalized intensity versus temperature curves have the same shape for all harmonics. This indicates a complete squaring up of the LRO magnetic structure in the whole temperature range below  $T_N$ .

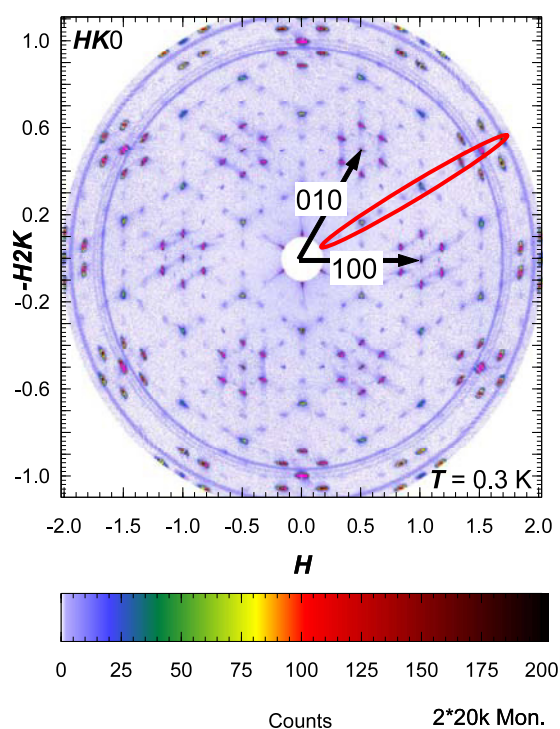


**Figure 6.** Full reciprocal  $HK0$  plane of  $\text{Er}_2\text{PdSi}_3$  at 300 mK. The reciprocal lattice vectors (010) and (100) are depicted with black arrows. A section of the long range ordered magnetic structure (circled) is shown in figure 7.

### 3.3. $\text{Er}_2\text{PdSi}_3$ : neutron diffraction

Figure 6 shows the reciprocal ( $HK0$ ) plane of  $\text{Er}_2\text{PdSi}_3$  at  $T = 0.3$  K. This reciprocal plane contains the nuclear reflections (100), (200) and (110). Two rings originate from scattering on polycrystalline copper (sample holder). The positions of the magnetic reflections correspond to a magnetic propagation vector of  $\tau = (1/9 \ 1/9 \ 0)$ . The magnetic moments are aligned along the hexagonal  $c$  axis deduced from the intensity distribution measured in ( $HHL$ ) scattering geometry. As for the  $\text{Tb}_2\text{PdSi}_3$  compound, LRO magnetic intensity is observed at the lowest temperature. But in contrast to the  $\text{Tb}_2\text{PdSi}_3$  case, no magnetic SRO is observed below  $T_N$ . Figure 7 shows a section of the reciprocal plane at  $T = 0.3$  K along the ( $HH0$ ) direction. The intensity relation between the different odd harmonics (1/9, 3/9 and 7/9) indicates a squared-up modulation of the magnetic moments.

An exception are the magnetic satellites near the positions where the (fourth and) fifth harmonics are expected. These magnetic satellites can be indexed with (0.434 0.434 0) and (0.562 0.562 0) instead of (4/9 4/9 0) and (5/9 5/9 0), respectively. Conditional upon the propagation vector the odd and even harmonics (if present) are on the same position.

Figure 8 shows the temperature dependence of the antiferromagnetic satellites. The temperature dependence of the first harmonic is drastically different from that of the other satellites. While the first harmonic is present over the whole magnetically ordered temperature range below  $T_N = 7$  K the other satellites are observed only below 5 K. Their intensity increases steadily with decreasing temperature in an upturned curvature until saturation is reached around 2 K, corresponding to the characteristic temperature  $T_2$  found in the ac susceptibility.

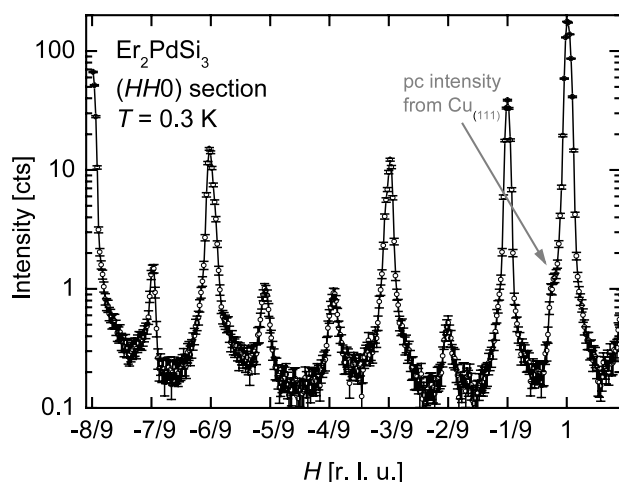


**Figure 7.** Section of the magnetic structure of  $\text{Er}_2\text{PdSi}_3$  as marked in figure 6. The magnetic satellites originating from the (110) reflection are numbered. Magnetic satellites originating from (000) are on the same positions. Note the logarithmic intensity scale.

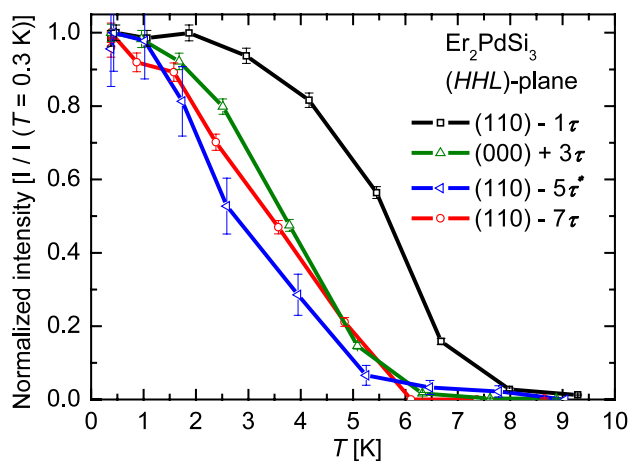


**Figure 8.** Normalized intensity for the different harmonics of the magnetic propagation vector of  $\text{Er}_2\text{PdSi}_3$ .

From these facts it can be concluded that  $\text{Er}_2\text{PdSi}_3$  first enters a simple sinusoidal antiferromagnetic phase below  $T_N$  while, upon lowering the temperature, the magnetic structure squares up continuously down to  $T_2$ . In the temperature range between 0.3 K and  $T_N$  all magnetic intensity is of LRO type. Therefore, the SGL transition found in the ac susceptibility at  $T_2$  is solely connected to the full squaring up of the magnetic structure.

#### 4. Conclusions and discussion

Two  $\text{R}_2\text{PdSi}_3$  ( $\text{R} = \text{Tb}, \text{Er}$ ) compounds which exhibit apparently similar SGL behaviours in macroscopic measurements were investigated using neutron diffraction. Both compounds show a squared-up long range antiferromagnetic order at lowest temperatures.



In  $\text{Tb}_2\text{PdSi}_3$  the antiferromagnetic LRO is squared up over the whole temperature range below  $T_N$ . All magnetic satellites of the LRO have a similar temperature dependence. No features of the LRO can be correlated with the temperature  $T_2$  of the additional phase transition. However, antiferromagnetic SRO with a characteristic temperature of  $T_2 \approx 8$  K was found. Thus, the disorder to SRO transition correlates with the observed SGL phase transition. The SRO is likely to originate from geometric frustration of magnetic moments which are not able to fulfil the antiferromagnetic coupling to all neighbours simultaneously. This frustration effect seems to affect the LRO arrangement only slightly.

In contrast to  $\text{Tb}_2\text{PdSi}_3$ ,  $\text{Er}_2\text{PdSi}_3$  does not show any magnetic SRO in the temperature region below  $T_N$  down to the lowest temperature. The measured intensities of the LRO harmonics of the propagation vector have a distinct temperature dependence, indicating a continuous squaring up of the antiferromagnetic order between  $T_N$  and  $T_2$ . The characteristic temperature in the intensity versus temperature curve of the higher harmonics is  $T_2 = 2$  K when saturation is reached. Therefore, the SGL transition in  $\text{Er}_2\text{PdSi}_3$  can be correlated with the full squaring up of the magnetic structure. We are not aware of publications where the frequency dependence of magnetic phase transitions from sine to squared-up modulation had been investigated.

In consequence, the investigation of  $\text{R}_2\text{PdSi}_3$  ( $\text{R} = \text{Tb}, \text{Er}$ ) compounds allowed us to deduce different strategies of magnetic systems to overcome frustration. Consequently, the magnetic moments of all  $\text{R}^{3+}$  ions should completely order below  $T_2$ . In  $\text{Tb}_2\text{PdSi}_3$  (with the moment direction within the basal plane) the formation of a SRO sublattice within the LRO magnetic structure is favoured. In  $\text{Er}_2\text{PdSi}_3$  (with the moment direction along the hexagonal axis) all magnetic moments are included in the LRO squared-up magnetic structure.

In principle, other compounds should behave similarly. However, other compounds of the  $\text{R}_2\text{PdSi}_3$  ( $\text{R} = \text{Ce}, \text{Dy}, \text{Ho}$ ) series do not show an additional phase transition in the interval between 1.5 K and  $T_N$ . Yet the published values [2] of the ordered magnetic moment (only half of the magnetic moment is ordered at  $T = 1.5$  K) and of the magnetic structure (only sine modulated) makes the existence of a second phase transition in the  $\text{Ce}_2\text{PdSi}_3$  and  $\text{Dy}_2\text{PdSi}_3$  compounds likely. Theoretical considerations of the free energy [10] show that a sine-modulated structure is not stable at  $T = 0$  for Kramers ions (such as  $\text{Ce}^{3+}$  and  $\text{Dy}^{3+}$ ). Therefore, a squaring up with an additional phase transition below  $T_N$  is possible (also see [11] for other examples). It would be interesting if this transition could be found in an accessible temperature region. We also plan to expand the single-crystal neutron diffraction to very low temperatures and investigate the magnetic structure of  $\text{Ho}_2\text{PdSi}_3$ .

## Acknowledgments

We gratefully acknowledge the scientific and experimental support from the people at the HMI and FRM-II research facilities. The investigation of  $\text{R}_2\text{PdSi}_3$  compounds is funded by the DFG through the research project SFB 463.

## References

- [1] Kotsanidis P A, Yakinthos J K and Gamari-Seale E 1990 *J. Magn. Magn. Mater.* **87** 199
- [2] Szytula A, Hofmann M, Penc B, Ślaski M, Majumdar S, Sampathkumaran E V and Zygmunt A 1999 *J. Magn. Magn. Mater.* **202** 365
- [3] Frontzek M, Kreyssig A, Doerr M, Rotter M, Behr G, Löser W, Mazilu I and Loewenhaupt M 2006 *J. Magn. Magn. Mater.* **301** 398
- [4] Paulose P L, Sampathkumaran E V, Bitterlich H, Löser W and Behr G 2003 *Phys. Rev. B* **67** 212401

- [5] Iyer K, Paulose P L, Sampathkumaran E V, Frontzek M, Kreyszig A, Doerr M, Loewenhaupt M, Mazilu I, Löser W and Behr G 2005 *Physica B* **355** 158
- [6] Li D X, Nimori S, Shiokawa Y, Haga Y, Yamamoto E and Onuki Y 2003 *Phys. Rev. B* **68** 012413
- [7] Frontzek M, Kreyszig A, Doerr M, Hoffman J-U, Hohlwein D, Bitterlich H, Behr G and Loewenhaupt M 2004 *Physica B* **350** e187
- [8] Graw G, Bitterlich H, Löser W, Behr G, Fink J and Schultz L 2000 *J. Alloys Compounds* **308** 193
- [9] Mazilu I, Frontzek M, Löser W, Behr G, Teresiak A and Schultz L 2005 *J. Cryst. Growth* **275** e103
- [10] Elliott R J 1961 *Phys. Rev.* **124** 346
- [11] Gignoux D and Schmitt D 1991 *J. Magn. Mater.* **100** 90